RAMAN SHIFTING HIGH POWER NEAR INFRARED LASER RADIATION

Dr. Wolfgang Rudolph
Dr. Jack McIver

Physics Department, University of New Mexico
800 Yale Blvd NE
Albuquerque, NM 87131

June 2001

Final Report

20011031 118

AIR FORCE RESEARCH LABORATORY
Directed Energy Directorate
3550 Aberdeen Ave SE
AIR FORCE MATERIEL COMMAND
KIRTLAND AIR FORCE BASE, NM 87117-5776

This report has been reviewed by the Public Affairs Office and is releasable to the National Technical Information Service (NTIS). At NTIS, it will be available to the general public, including foreign nationals.

If you change your address, wish to be removed from this mailing list, or your organization no longer employs the addressee, please notify AFRL/DELC, 3550 Aberdeen Ave SE, Kirtland AFB, NM 87117-5776.

Do not return copies of this report unless contractual obligations or notice on a specific document requires its return.

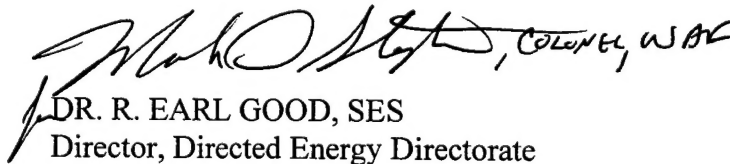This report has been approved for publication.

BRIAN T. ANDERSON, DR-2
Project Manager

FOR THE COMMANDER

JOHN C. DEL BARGA, MAJ, USAF   DR. R. EARL GOOD, SES
Chief, High Power Gas Lasers Branch   Director, Directed Energy Directorate

REPORT DOCUMENTATION PAGE

Form Approved
OMB No. 0704-0188

1. REPORT DATE *(DD-MM-YYYY)*	2. REPORT TYPE	3. DATES COVERED *(From - To)*
10-06-2001	Final	02/27/98 - 05/31/01

4. TITLE AND SUBTITLE	
Raman Shifting High Power Near Infrared Laser Radiation	**5a. CONTRACT NUMBER** F29601-98-K-0038
	5b. GRANT NUMBER
	5c. PROGRAM ELEMENT NUMBER 62601F

6. AUTHOR(S)	
W. Rudolph and J. McIver	**5d. PROJECT NUMBER** 3326
	5e. TASK NUMBER LA
	5f. WORK UNIT NUMBER 02

7. PERFORMING ORGANIZATION NAME(S) AND ADDRESS(ES)	8. PERFORMING ORGANIZATION REPORT NUMBER
Physics Department, University of New Mexico 800 Yale Blvd NE Albuquerque, NM 87131	2001-02

9. SPONSORING / MONITORING AGENCY NAME(S) AND ADDRESS(ES)	10. SPONSOR/MONITOR'S ACRONYM(S) AFRL/DELC
	11. SPONSOR/MONITOR'S REPORT NUMBER(S) AFRL-DE-TR-2001-1041

12. DISTRIBUTION / AVAILABILITY STATEMENT

Approved for public release; distribution is unlimited.

13. SUPPLEMENTARY NOTES

14. ABSTRACT

Raman scattering for efficient wavelength conversion of mid infrared radiation was investigated theoretically and experimentally. Conversion efficiencies as high as 70 % were observed with stimulated Raman scattering in H_2. Several conversion schemes were analyzed theoretically and their applicability for the conversion of iodine lasers was investigated. The most efficient configuration uses a synchronously pumped Raman laser. For this technique, the single pulse of the iodine laser must be converted into a train of short (ns) pulses.

15. SUBJECT TERMS
Stimulated Raman scattering, Raman lasers, nonlinear optics, iodine laser

16. SECURITY CLASSIFICATION OF:			17. LIMITATION OF ABSTRACT	18. NUMBER OF PAGES	19a. NAME OF RESPONSIBLE PERSON Brian T. Anderson
a. REPORT U	b. ABSTRACT U	c. THIS PAGE U	unlimited	20	19b. TELEPHONE NUMBER *(include area code)* (505) 846-4748

Standard Form 298 (Rev. 8-98)

i

Table of Contents

List of Figures

1. Introduction

The main goal of this project was to explore efficient frequency conversion of iodine lasers emitting pulses of microsecond duration and energies of several Joule using stimulated Raman scattering (SRS). Alternatively the laser can be modelocked producing a microsecond train of pulses of 1-3 ns duration. These two possible pump scenarios are rather different as they encompass stationary and nonstationary Raman scattering. Moreover, in the modelocked case, the single pulse intensity is not likely to be high enough to overcome the SRS threshold. That makes it necessary to explore various Raman laser configurations. The expected iodine laser parameters were as follows:

regime	pulse duration	pulse energy	pulse power
regime 1	3 µs	1-10 J	0.3-3 MW
regime 2	1-3 ns	3- 30 mJ	1-30 MW

Because of the damage behavior of solids and the heat load resulting from the high-energy pump laser our effort focused on gases as Raman material. For the desired frequency shift from $\lambda_0 = 1.315$ µm to $\lambda_S = 1.4 - 1.5$ µm rotational SRS in hydrogen ($\lambda_S = 1.43$ µm) was chosen. In addition, H_2 exhibits one of the largest Raman cross sections.

During the project an iodine laser was not available and the experiments were carried out with a Nd:YAG laser operating at 1.06 µm. Even though the energies and pulse durations are rather different than those from iodine lasers our combined theoretical and experimental study allows us to draw relevant conclusions.

2. Theoretical Results

2.1 Extracavity Conversion

Rotational SRS involves the interaction of a pump laser field and a material excitation (rotational energy ΔE) to produce frequency-shifted (Stokes) radiation, see Fig.1.

$$J \rightarrow J+2$$

$$\Delta E \approx 4hcB\left(J + \frac{3}{2}\right)$$

$$B \approx \frac{h}{8\pi^2 cR^2}\frac{m+M}{mM}$$

H_2: $B = 59.34$ cm^{-1}

$\Delta E (J=0) = 354$ cm^{-1} para

$\Delta E (J=1) = 587$ cm^{-1} ortho
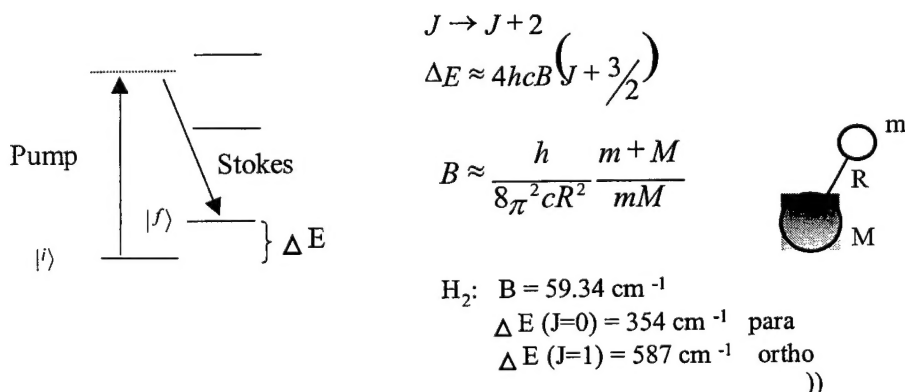
Fig.1: *Schematic diagram of rotational Raman scattering in a diatomic molecule with nuclear masses of m and M (m = M = 1.7 10^{-27} kg for H_2) and nuclear separation R.: The scattering process excites the molecule from a rotational level J to level J+2. Because of its greater abundance only ortho-H_2 will be considered. At room temperature the J=1 level is mostly populated (66 %) which results in the listed Raman shifts. Due to momentum conservation a circularly polarized pump is needed to mediate this transition.*

In the simplest case a pump of constant intensity I_p propagates through a Raman medium of length L generating Stokes radiation of intensity I_s. Neglecting pump depletion and transient effects SRS is described by the following equation:

$$I_s(L) = I_{s0} e^{G_s} \qquad (1)$$

where

$$G_S = g_s I_{P0} L \qquad (2)$$

is the Raman gain with g_S being the Raman gain coefficient and I_{S0} is either noise input at the Stokes frequency or the intensity of a Stokes seed. It is common to define the Raman threshold by $G_S = 30$. For rotational scattering in H_2, $g_s \approx 1$ cm/GW.

To estimate the feasibility of extracavity SRS with the microsecond iodine pulse let us now consider a focused beam with the beam waist (radius w_0) located in the center of the Raman medium. In this case the exponent in Eq. (1) becomes

$$G_s = \frac{2}{\lambda} g P_p \arctan\left(\frac{L}{2L_c}\right) \qquad (3)$$

where L_c is the Rayleigh range and P_p is the pump power. Because of the arctan function increasing the crystal length from $2L_c$ to infinity increases the gain coefficient only by a factor of two. For practical reasons we will therefore assume a cell of length $L = 2L_c$ for which

$$G_s = \frac{\pi}{2\lambda} g P_p. \qquad (4)$$

The minimum pump power required to reach the threshold for SRS can be obtained from Eq. (3) by setting $G = 30$:

$$P_{min} \approx \frac{20\lambda}{g}$$

which results in $P_{min} = 2$ MW for H_2. With 3 μs, 10 J pulses we obtain a power of 3 MW. This just barely exceeds the theoretical threshold for SRS. In practice it is therefore doubtful that extracavity scattering is feasible. Another practical limitation is the beam parameter of the iodine laser. The best-case scenario assumed here requires the cell length to be at least equal to the confocal length. Poor focusing capabilities of the laser mean very long gas cells. For these reasons Raman laser concepts were explored.

SRS is typically divided into two different regimes - (i) stationary and (ii) nonstationary scattering. The stationary case occurs when the pump pulse duration $\tau \gg G_S T_2$, where $T_2 = (\pi \Delta \nu)^{-1}$ is the phase relaxation time of the transition and $\Delta \nu$ is the Raman line width. In this case the Raman conversion can be described by rate equations for the pump and Stokes intensities.

$$\frac{d}{dz}I_S = g_S I_P I_S$$

$$\frac{d}{dz}I_P = -\frac{\nu_P}{\nu_S} g_S I_P I_S \tag{5}$$

where $\nu_{P,S}$ is the pump and Stokes frequency, respectively. Without depletion of the pump this set of equations has the solution (1). With pump depletion the solution is

$$I_{S,P}(z) = \frac{K\nu_{S,P}}{1 + \dfrac{\nu_{S,P}}{\nu_{P,S}} \dfrac{I_{P0,S0}}{I_{S0,P0}} \exp(-G_S \nu_P K z)} \tag{6}$$

where

$$K = \frac{I_{P0}}{\nu_P} + \frac{I_{S0}}{\nu_S}.$$

Further equations need be added to Eqs. (5) if higher order Stokes processes occur. Figure 2 shows the qualitative behavior of the solution of Eq. (4) in the presence of higher Stokes generation.
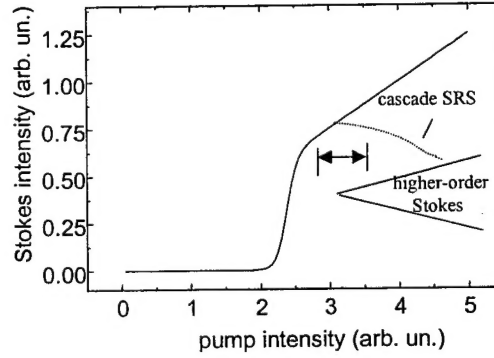
Fig.2: *Qualitative behavior of Stokes generation as a function of pump intensity.*

For maximum first Stokes generation there is a relatively small window of pump intensities above the SRS threshold. If the pump is too intense higher-order Stokes production starts to deplete the first Stokes.

The nonstationary or transient regime is more complicated to deal with as the transient response of the material has to be considered. The coupled equations for the pump and Stokes electric field $E_{P,S}$ and the normal mode material excitation Q read

$$\frac{\partial E_S}{\partial z} + \frac{1}{\nu_S}\frac{\partial E_S}{\partial t} = \kappa_S E_P Q^*$$

$$\frac{\partial E_P}{\partial z} + \frac{1}{\nu_P}\frac{\partial E_P}{\partial t} = \kappa_P E_S Q \tag{7}$$

$$\frac{\partial Q}{\partial t} + \pi\Delta\nu Q = \kappa_Q E_P^* E_S$$

3

where $\kappa_j = i\dfrac{\mu_0 cN\omega_i}{4}\dfrac{\delta\alpha}{\delta q}$ and j stands for Stokes (s) or pump (p), $\kappa_Q = i\dfrac{1}{4\mu_0\omega_p N}\dfrac{\delta\alpha}{\delta q}$

where $\dfrac{\delta\alpha}{\delta q}$ is the derivative of the polarizability with respect to the vibration coordinate.

In general this set of equations has to be solved numerically, in particular if higher-order Stokes generation occurs. Figure 3 shows a qualitative comparison of stationary and nonstationary Raman scattering in the transient limit ($\tau \ll T_2$).

It is obvious that the Raman gain and conversion is reduced in the transient regime making it more difficult to work with short pulses. There exists no comprehensive theoretical study of transient Raman scattering that is applicable to the situation of interest here. Therefore part of our effort was devoted to develop such a theory and to analyze rotational Raman scattering in H_2 quantitatively. The model consists of a plane pump field propagating in the positive z-direction while inducing SRS. We consider the production of Stokes radiation up to the 3rd order and anti-Stokes generation up to order one (index AS). The set of partial differential equations that governs this scenario is

Fig. 3: *Calculated transient gain versus stationary gain.*

$$\left(\frac{1}{c}\frac{\partial}{\partial t}+\frac{\partial}{\partial z}\right)E_{1AS} = i\kappa_{1AS}QE_p$$

$$\left(\frac{1}{c}\frac{\partial}{\partial t}+\frac{\partial}{\partial z}\right)E_p = i\kappa_p\left(Q^*E_{1AS}+QE_p\right)$$

$$\left(\frac{1}{c}\frac{\partial}{\partial t}+\frac{\partial}{\partial z}\right)E_{1S} = i\kappa_{1S}\left(Q^*E_p+QE_{2S}\right) \qquad (8)$$

$$\left(\frac{1}{c}\frac{\partial}{\partial t}+\frac{\partial}{\partial z}\right)E_{2S} = i\kappa_{2S}\left(Q^*E_{1S}+QE_{3S}\right)$$

$$\left(\frac{1}{c}\frac{\partial}{\partial t}+\frac{\partial}{\partial z}\right)E_{3S} = i\kappa_{3S}Q^*E_{2S}$$

$$\left(\frac{\partial}{\partial t}+\frac{1}{T_2}\right)Q = -i\kappa_Q\left(E_{1AS}E_p^*+E_pE_{1S}^*+E_{1S}E_{2S}^*+E_{2S}E_{3S}^*\right)$$

These equations were solved numerically for a variety of experimental situations and the results were compared to stationary SRS. A detailed account of the simulation is attached in the Appendix. Here we concentrate on the main aspects pertinent to the experiments. Figure 4 illustrates cascade scattering in the transient regime. Compared to stationary scattering (cf. Fig.2) with the same pump intensity, the transient interaction reduces the conversion efficiency. In both cases there is a parameter range where only 1st Stokes radiation exists.
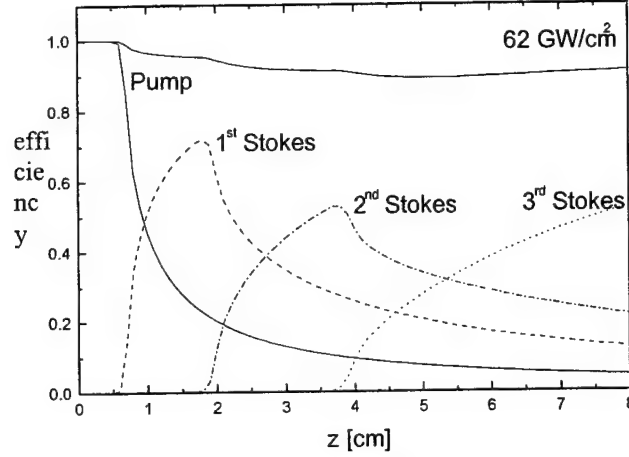
Fig. 4: *Transient cascade SRS of a 10 ns pulse. In the transient case T_2= 600 ps corresponding to 5 bar of H_2. A beam of constant intensity was assumed.*

Alternatively the interaction length can be adjusted so as to concentrate on a certain higher-order Stokes. This adjustment can be done by varying the confocal parameter (focused spot size) of the pump. In the transient regime, unlike in the stationary case, several higher order Stokes components coexist.

The shape of the produced Stokes and the depleted pump is distinctly different for the transient and stationary regime. Figure 5 depicts two examples. In the stationary case only the central part of the pulse where the SRS threshold is exceeded is depleted.
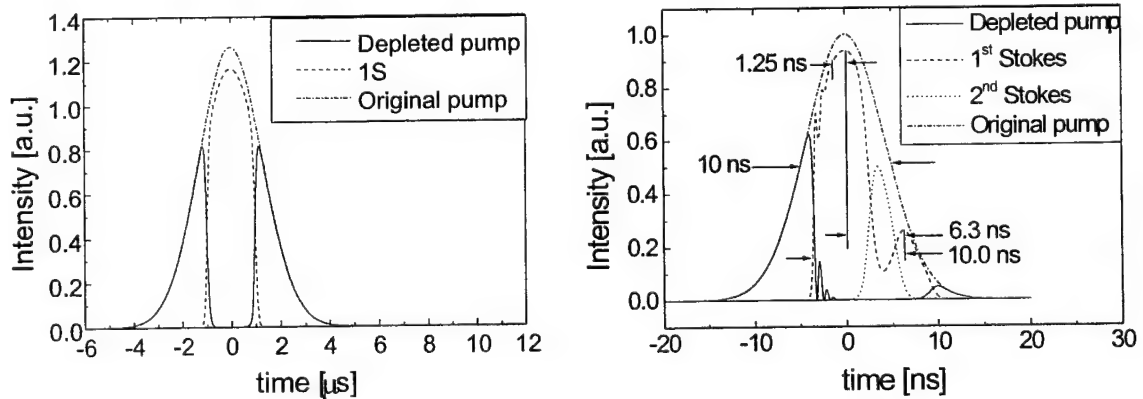
Fig. 5: *Comparison of pulse shapes for stationary (left, 10 J, 3 μs) and transient (right, 10 ns) Raman scattering (p = 5 bar).*

5

Transient SRS is associated with fast modulations of the pulse intensities. The general case of transient (rotational) scattering in H_2 involving higher-order Stokes generation and parametric processes is not treated in the literature. The appendix contains a detailed evaluation of this case. To verify some of our theoretical predictions we recorded Raman pulses (1st Stokes) with a 10 ps streak camera. An example is shown in Fig.6. The transient oscillations are clearly visible and are in good quantitative agreement with the theory.
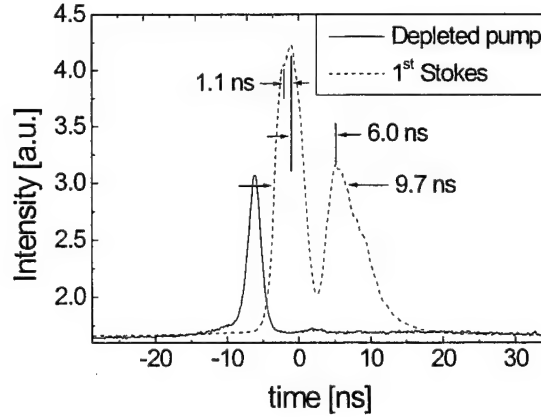
Fig. 6: *Streak camera traces of the 1st Stokes pulse. The pump was a 10 ns Nd:YAG laser pulse converted via rotational SRS in H_2 (5 bar). The experimental curves compare well with theory (see previous the figure).*

In summary, depending on the operational mode of the iodine laser (modelocked or non-modelocked) transient and stationary Raman scattering have to be considered. The transient process is expected to result in a reduced conversion efficiency, higher threshold, and modulations in the converted pulse.

2.2 Raman Laser

There a number of possible laser and pump configurations that reduce the Raman threshold and at the same time can lead to an improved beam quality. Of the many possible configurations we focused on one scheme that seemed particularly interesting for the conversion of the iodine laser radiation. It consists of a cavity built around the Raman cell, see Fig.7. The pump is coupled into the cell through a dichroic beam splitter (DBS).

The mirror M_2 can be high-reflective for the pump to allow for a double pass and a better overall energy conversion. We investigated two different pump regimes -

Fig. 7: *Schematic diagram of an extracavity pumped Raman laser. The pump is either the 3 µs iodine pulse or a modelocked train of ns pulses. In the latter case we refer to the system as synchronously pumped laser.*

6

(i) where the pump is a 3 µs pulse and (ii) where the pump is a 3 µs train of modelocked pulses that have a duration of 1-3 ns each. Case (ii) is referred to as synchronously pumped Raman laser. To fully utilize its potentials the roundtrip time in the pump and Raman cavity have to match.

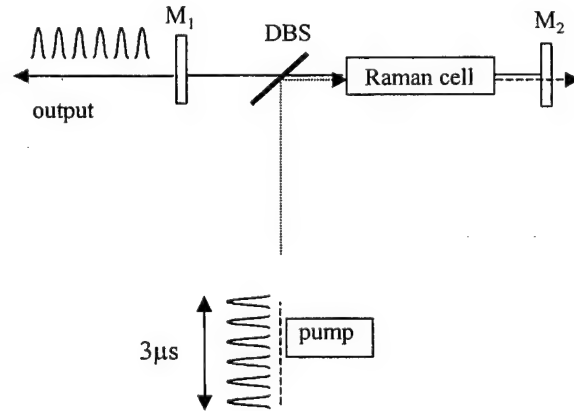The goal of our theoretical studies was to determine the Raman threshold reduction as compared with extracavity conversion and to predict the achievable conversion rates and pulse parameters in both regimes. One expects a threshold reduction in both cases as the resonating (albeit weak) Stokes produced by the leading edge of the pump pulse can act as seed for the conversion of subsequent parts of the pump.

The theoretical investigation was based on a roundtrip model for the laser that takes into account the mirror reflectivities and the temporal shape of the pump pulse (train). The interaction with the Raman medium was described using Eqs. (6).

Regime (i) - three microsecond pump pulse:

Figure 8 summarizes the results obtained for the Raman laser pumped by the 3 µs iodine pulse. The two graphs also show that by choosing the reflectivity of the laser outcoupler for 1st and 2nd Stokes one can select a certain Stokes component to be the dominant laser output. This is demonstrated here for up to the 2nd Stokes; with somewhat reduced efficiency this is also possible for higher-order Stokes lasers. For low pump intensities a certain minimum reflectivity of the outcoupler is necessary to reach the laser threshold. Compared to extracavity scattering (cf. Fig. 2) the Raman conversion is now possible at very reasonable pump beam diameters and cell lengths. The tolerance range for the focusing is also greater.
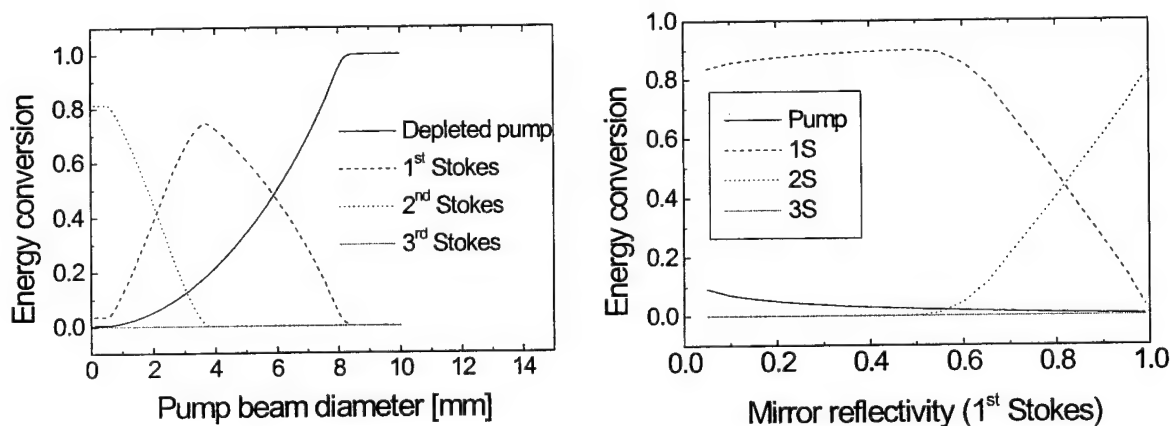
Fig. 8: *Theoretical Modeling of a Raman laser based on rotational scattering in H_2 and pumped by a 3 µs, 10 J iodine laser pulse. Left: conversion as a function of pump beam diameter, cell length 40 cm, $R_{1st}=0.99$. Right: Output as a function of the end mirror reflectivity R_{1st}. ($R_{2nd} = 0$).*

Regime (ii) - three microsecond train of 1-3 ns pulses

Modelocking the iodine laser results in an increase of the pulse peak power. This may be important for reaching the Raman threshold. On the other hand the transition from microsecond to nanosecond pump pulses means a transition from the stationary to the

7

transient regime and leads to the difficulties discussed above. To decide on the usefulness of modelocking and the synchronous pumping we performed a detailed numerical study. Its main results are summarized here. Additional data and their comparison with experiments conducted with a Nd:YAG laser can be found in the appendix.

The simulation refers to the laser schema depicted in Fig.7. A train of pulses (1 ns duration each) with a Gaussian 3 µs envelope pumps the gas cell. An important parameter is the length mismatch between the Raman laser length and the pump pulse separation ΔL. While the mismatch must not be greater than a pump pulse length the exact optimum for maximum conversion efficiency needs to be determined. Figure 9
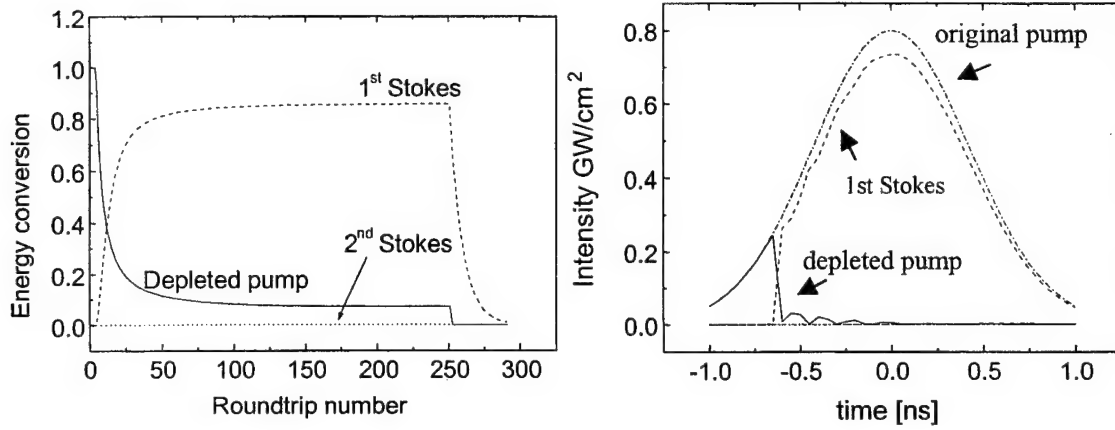

Fig. 9: *Energy of various Stokes pulses as a function of roundtrip number (left). The pump was a train of 250 (Gaussian) pulses with a rectangular envelope. The picture on the right illustrates the depletion of an individual pump pulse in the later part of the train. (reflectivity of the end mirror $R_{1st}=0.8$ and $R_{2nd}=0$)*

shows the evolution of the Stokes pulse train. After about 25 roundtrips (25 pump pulses) the Stokes pulse is fully developed corresponding to an energy conversion of about 80%. The original pump pulse is almost fully depleted for this case. For simplicity the pump envelope was assumed to be of rectangular shape; simulations with more physical shapes resulted only in small quantitative changes.

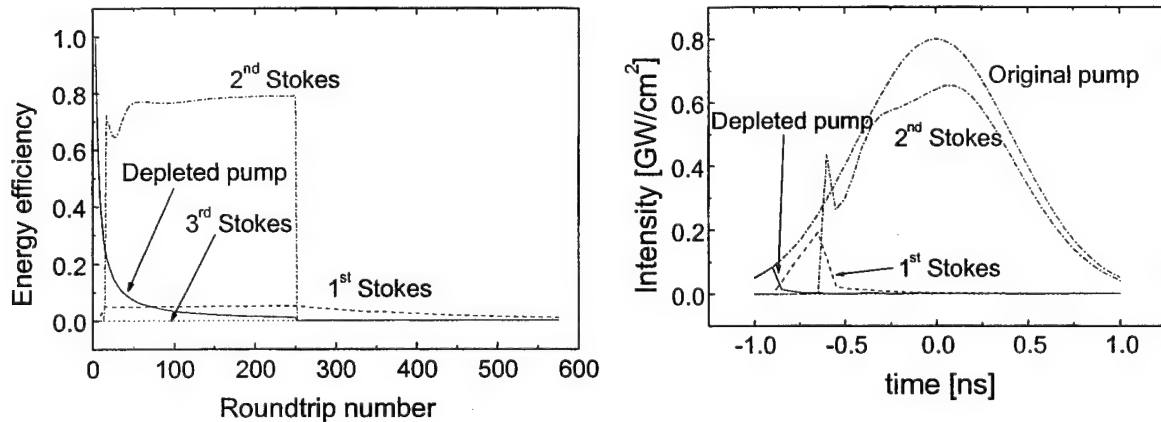**Fig. 10:** *Energy of various Stokes pulses as a function of roundtrip number (left). The pump was a train of 250 (Gaussian) pulses with a rectangular envelope. The right figure illustrates the depletion of an individual pump and 1st Stokes pulse in the later part of the train.(reflectivity of the end mirror $R_{1st}=0.99$ and $R_{2nd}=0.72$). A 10 J pump pulse (train) focused to 1.3 mm was used.*

8

Like in case (i) it is possible to switch between various Stokes outputs by changing the reflectivity of the outcoupler. This is exemplified in Fig.10.

With low losses for the 1st Stokes radiation the second Stokes immediately after the Raman laser reaches threshold starts to build up and is coupled out. Likewise an increase of the mirror reflectivity for the 2nd Stokes in addition to low losses for the 1st Stokes will result in output of the 3rd Stokes component.
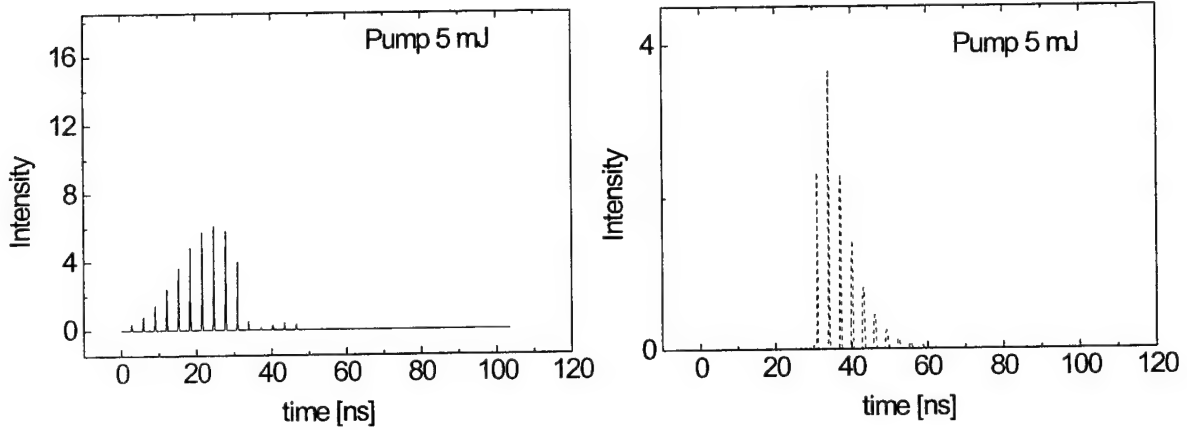

Fig. 11: *Depleted Nd:YAG pump and 1st Stokes pulse train.*

       Since our experiments were conducted with a Nd:YAG laser we also simulated the situation of a short pulse train. Figure 11 shows the undepleted and depleted pump train together with the first Stokes pulse. As expected, the Raman pulse is produced delayed with respect to the pump pulse train. Once it has reached a certain level the pump is depleted, resulting in high-energy conversion in the second half of the pump train.

An important feature of a synchronously pumped Raman laser is the dependence of the output on the length mismatch of pump and Raman cavity. This was calculated for two different numbers of pulses in the pump train. The total energy of the train was kept constant at 15 mJ. The results are shown in Fig.12. The shift of the optimum mismatch with decreasing pulse number, that is increasing energy of an individual pulse, is a result
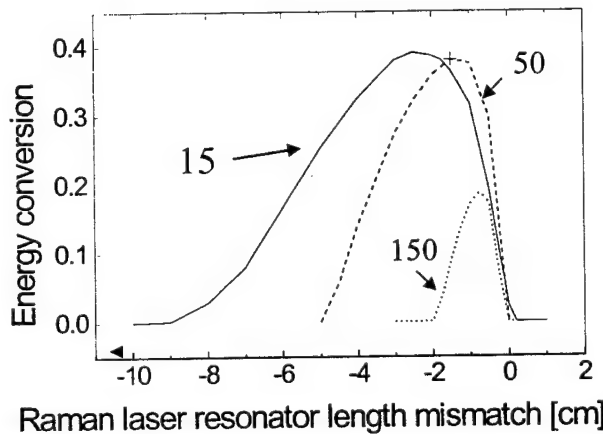

Fig. 12: *Raman convertsion as a function of the length mismatch of pump and Raman laser for different number of pump pulses in the pump train. The total energy of the pulse train was kept constant.*

of the transient scattering of the 200 ps Nd:YAG pulses.

In summary, Raman lasing can decrease the conversion threshold and allows for the generation of specific higher-order Stokes components. The following table summarizes the thresholds for extracavity and Raman conversion for the 3 μs pulse and the modelocked train. The threshold data were normalized to the synch. pumped case. For the pump we used 10 J pulse (train) focused to 1.3 mm. The duration of the modelocked pulses was assumed to be 1 ns. The results were essentially identical for pulse durations between 1 and 5 ns.

	normalized threshold energy		energy conversion	
regime	extracavity	Raman laser	extracavity	Raman laser
3 μs pulse	627	1.7	0.7	0.9
3 μs pulse train	304	1	0.5	0.8

Clearly, in terms of threshold, the laser architectures are favored. The synchronously pumped laser shows the lowest thresholds of all.

3. Experimental Results

3.1 Extracavity Experiments

The layout of the extracavity Raman conversion experiment is sketched in Fig.13. The output of a Q-switched Nd:YAG laser (τ = 10 ns) was circularly polarized and coupled into a 75 cm cell filled with H_2 at a pressure p. The output radiation was spectrally dispersed and monitored with an energy meter. The Raman conversion is rather independent of the exact focusing as long as the confocal parameter is not longer than the cell and gas break down does not occur.
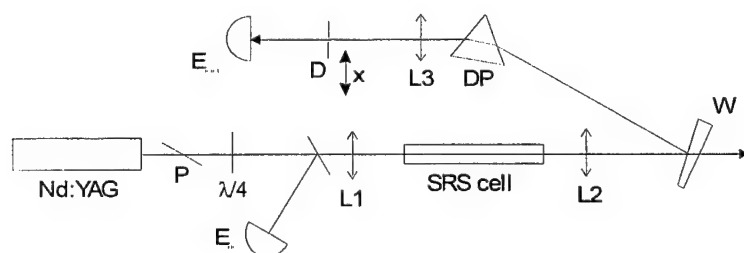

Fig. 13: *Schematic diagram of extracavity Raman conversion of pulses from a Q-switched Nd:YAG laser at 1.06 μm. The focal length of lens 1 and 2 was 50 cm.*

The energy conversion into Stokes radiation and the pump transmittance through the cell were measured as a function of the gas pressure for various pump intensities in the focus. The results are depicted in Fig.14.
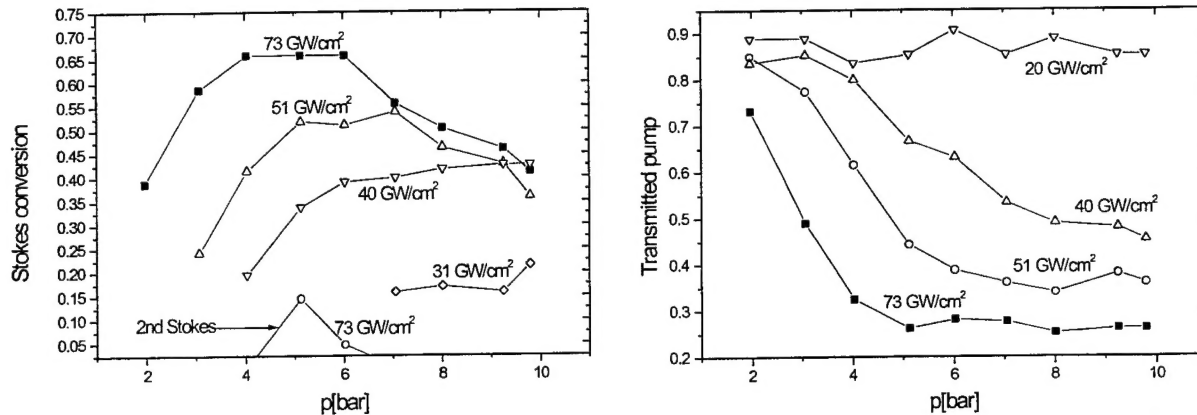
Fig. 14: *Energy conversion (left) and pump transmittance (right) as a function of gas pressure.*

The Raman threshold was at about 25 GW/cm^2. At about 70 GW/cm^2, the 1st Stokes component reaches a maximum and a small 2nd Stokes pulse appears. Increasing the pump intensity beyond that value does not increase the 1st Stokes but rather leads to higher order Stokes radiation at the expense of the 1st Stokes (cf. Fig. 2). The optimum gas pressure was about 5 bar. Strong Raman conversion is associated with pump depletion as documented in the figure to the right. From these experiments one can predict that conversion of the non-modelocked iodine laser pulse is only marginally feasible. To reach the 30 GW/cm^2 one would have to focus the iodine laser beam to a spot smaller than 100 μm which is experimentally very challenging.

3.2 Raman Laser

In cases where the Raman threshold cannot be reached Raman lasing and/or intracavity Raman pumping may be of advantage. Because of the lack of an iodine laser we performed the experiments with a Q-switched Nd:YAG laser. We explored several concepts to modelock and stretch the pulse train. The results are summarized in Fig.15.

The longest pulse trains were observed with negative feedback and with the free-running laser. However, the pulse energy (per modelocked pulse) was too low to make meaningful SRS experiments. We therefore decided to work with the Q-switched and modelocked pulse train. Modelocking was achieved by placing an acousto-optic modulator in the YAG resonator (65 MHz). The resulting 50 ns pulse train with a 7.3 ns pulse separation does not mimic the microsecond train from the iodine laser, but it should allow for a proof of principle. It should be noted that the Raman conversion of a short pulse train is more difficult (cf. Fig.12). Moreover the YAG laser produced a train of 200 ps pulses which unlike the 1-3 ns pulses expected from the modelocked iodine laser fall into the transient limit of SRS.
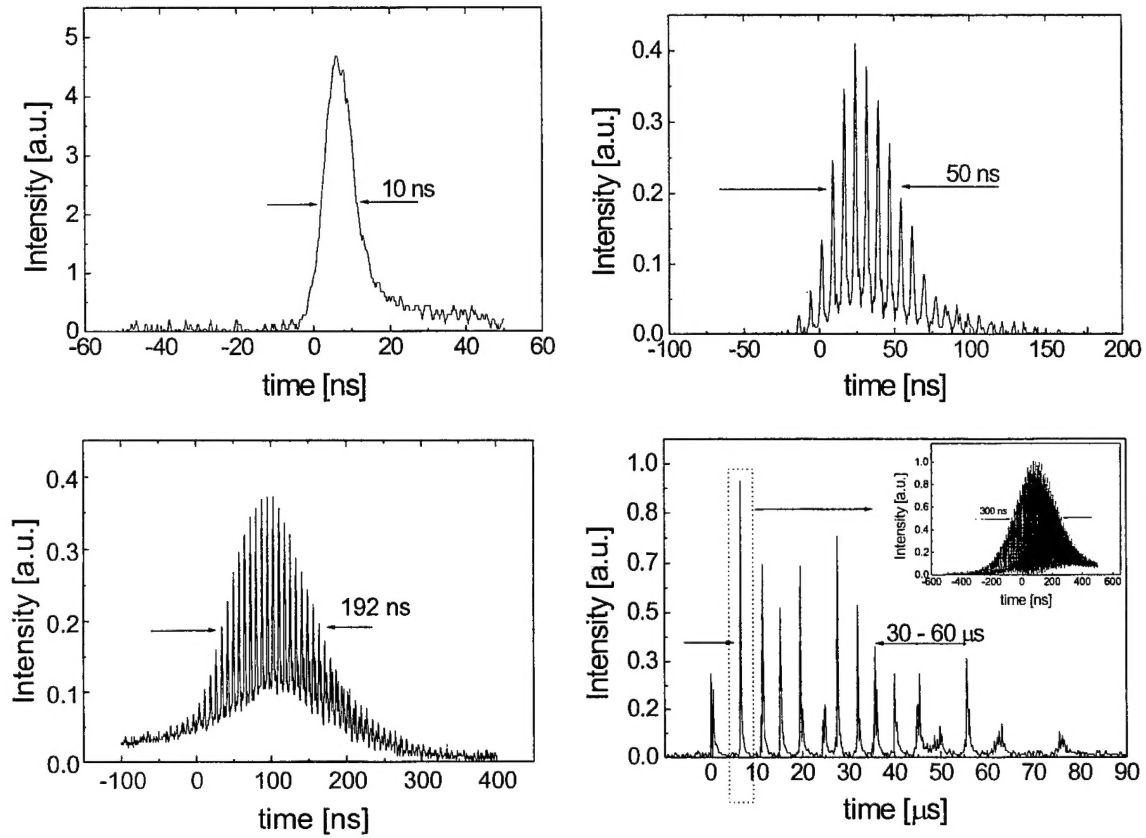
11

Fig. 15: *Pulses from a Nd:YAG laser. From top left: Q-switched; Q-switched and modelocked; Q-switched, modelocked and negative feedback (GaAs); free-running and modelocked.*

Figure 16 shows a schematic diagram of the setup of the synchronously pumped H_2 Raman laser. The pump energy in the pulse train was about 20 mJ and the focal length of the two lenses about 30 cm. The mirrors were flat. When aligned optimally the threshold for Raman lasing (10 mJ) was about four times lower than the threshold for extracavity scattering (40 mJ). This reduction factor is in qualitative agreement with theory. Note that
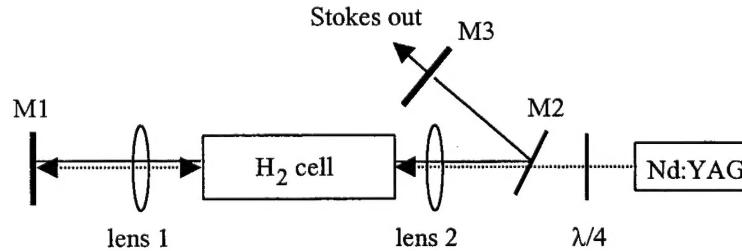

Fig. 16: *Schematic diagram of a Raman laser synchronously pumped by a train of about 10 pulses of a Nd:YAG laser. The mirror M1 has a maximum reflectivity for both the Nd:YAG and the Stokes radiation. Mirror M3 acts as the outcoupler for the Raman laser. The lens separation is adjusted to ensure a stable Stokes cavity.*

12

because of the shortness of the pump pulse train the threshold reduction factors of table 1 do not apply here. The maximum conversion efficiency to first Stokes radiation was 35%, which is also within the range suggested by theory (45%). The features of synchronous pumping are illustrated in Fig.17. The Raman laser output as a function of the length mismatch of pump and Raman laser is shown. The region where lasing occurs has about the length of the pump pulse. Optimum conversion occurs when the Raman laser is shorter than the pump laser. The reason is the delayed response of the Raman medium in the transient regime (cf. Fig. 5).

Conversion is only possible if the length mismatch is smaller than the pump pulse duration (about 200 ps). The laser is below threshold if pump and circulating Stokes pulse do not overlap in the active medium. The Stokes pulse occurs delayed with respect to the pump train. This is expected since the pump intensity is below the threshold for extracavity scattering.
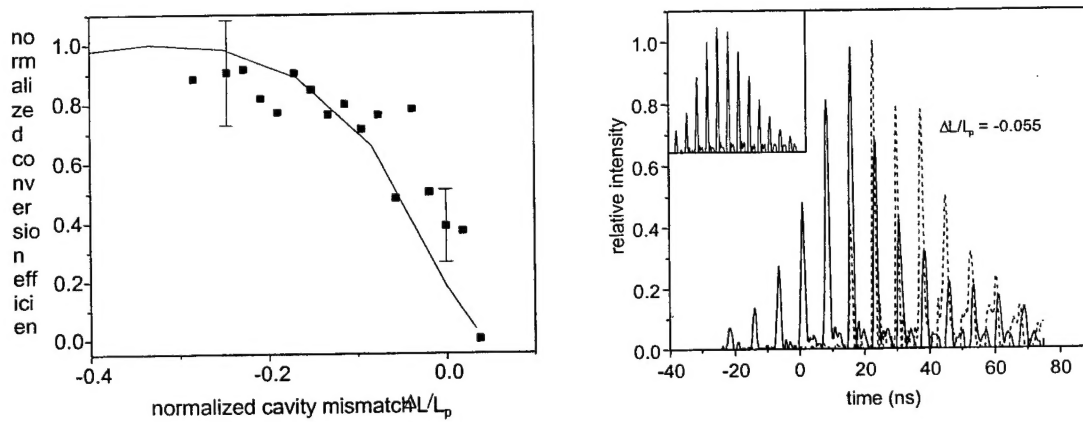

Fig. 17: *Left: Raman output as a function of the length mismatch of pump and Raman laser. Right: depleted pump pulse train (solid line) Stokes pulses (dashed line). The inset shows the undepleted pump train.*

4. Summary

Raman shifting of microsecond pulses from iodine lasers with energies > 5 J in gases was investigated theoretically. Experiments were conducted with Nd:YAG lasers to demonstrate the feasibility of some of the suggested conversion schemas. While extracavity conversion is a possibility, the most promising configurations that allow for some experimental error involve a Raman laser. The laser can be pumped either by the 3 microsecond iodine pulse or by a 3 microsecond train of modelocked pulses. The latter laser configuration (synchronously pumped Raman laser) is particularly promising as it has the lowest Raman threshold of all schemas tested. This concept was demonstrated, to the best of our knowledge for the first time, using a modelocked and Q-switched Nd:YAG laser. The single pulse power of the Nd:YAG laser was comparable to that of the modelocked iodine laser while its pulse duration and pulse train were 5-10 times shorter and 50 times shorter, respectively.

DISTRIBUTION LIST

DTIC/OCP
8725 John J. Kingman Rd, Suite 0944
Ft Belvoir, VA 22060-6218   1 cy

AFSAA/SAMI
1570 Air Force Pentagon
Washington, DC 20330-1570   1 cy

AFRL/VSIL
Kirtland AFB, NM 87117-5776   2 cys

AFRL/VSIH
Kirtland AFB, NM 87117-5776   1 cy

Physics Department, University of New Mexico
800 Yale Blvd NE
Albuquerque, NM 87131   1 cy

Official Record Copy
AFRL/DELC/Brian T. Anderson   3 cys